JOURNAL OF MATERIALS SCIENCE 31 (1996) 61–70

Analysis of elastic fibre bridging in the multiple cracked composite

J. KULLAA
VTT (Technical Research Centre of Finland), Building Technology, P.O. Box 1807, FIN-02044 VTT, Finland

A fibre pull-out problem in the multiple cracking stage is studied. Full bonding is assumed. When studying a single fibre the equilibrium condition may be violated at either of the cracks. Therefore to satisfy equilibrium a two-fibre system is assumed. Different cases were analysed and compared with the single fibre system. Also analysed was a case in which the two fibres partially overlap between two cracks; two examples are presented.

1. Introduction

In fibre-reinforced brittle matrix composites, the fibres are effective primarily in the post-cracking case. Under tension the composite may fail either in a single fracture mode, or after reaching a multiple cracking stage. The cracking mode depends on whether the fibres at the crack can sustain the total load needed for crack formation. In the multiple cracking stage the matrix is divided into segments of similar lengths. The matrix is stress-free at the edges of the cracks, and the load is carried by the fibres bridging the cracks. The stress-transferring mechanism from the fibres to the matrix has a considerable influence on crack spacing and width.

While in brittle matrix composites with continuous fibres pseudostrain-hardening occurs due to multiple cracking, composites with randomly oriented discontinuous fibres generally fail in a tension-softening mode upon the initiation of the first crack. However, it has been shown (e.g. Naaman and Shah [1], Tjiptobroto and Hansen [2]) that the multiple cracking stage can be achieved even with short fibres if the fibre volume content is sufficiently high. Moreover, Li and Leung [3] have presented analytical conditions for multiple cracking of a discontinuous random-fibre composite using a fracture mechanics approach.

The analytical treatment of the fibre bridging the crack in the multiple cracking stage differs somewhat from the theory of the pull-out test. In the pull-out test the boundary conditions are: at the fibre loaded end the fibre force is the same as the external load; at the embedded end the tensile stress in the fibre is usually assumed to be zero. In the multiple cracking case, the fibre may extend over two or more cracks if the crack spacing is sufficiently low. Because the matrix stress is zero at the crack, the shear stress between the fibre and the matrix is not continuous across the crack. Therefore the boundary conditions must be stated for the segment between the cracks.

In the case of continuous fibres, it can be assumed that the fibre force is equal to that at the adjacent crack. With short fibres the fibre's shorter embedded length at the crack may be too low to carry the load equal to that at the adjacent crack. Thus the fibre forces at the two cracks are not in balance. This is why when only a single fibre is studied the equilibrium condition may be violated.

It can be assumed that at the adjacent crack is another fibre located symmetrically with respect to the fibre being analysed [4]. The fibre force transfers from the fibre to the matrix and further to the other fibre. Then the forces in the two-fibre system at the cracks satisfy the equilibrium condition. The moment equilibrium condition can be assumed to be fulfilled statistically around the fibre.

With a single fibre the analysis leads to a second order differential equation for the fibre force with two boundary conditions [5]. With a two-fibre system it leads to a fourth order differential equation with four boundary conditions, as shown later.

The ACK model by Aveston and colleagues [6] assumed a uniform frictional shear stress between the continuous fibres and the matrix. Kullaa [4] used the same assumption in a statistical model of multiple cracking of a discontinuous fibre composite. In the present analysis full bonding between fibre and matrix is assumed. The main assumption needed for development of the model is the relationship between the interface shear stress and the local relative displacement between the fibre and the matrix. In the models by Naaman *et al.* [5], Nammur and Naaman [7], and Lim *et al.* [8], a linear relationship was chosen in the full bonded case. Stang *et al.* [9] modelled the matrix as a shear lag with a linear shear stiffness on a rigid support. An axially symmetric shear–lag model also leads to a linear relationship between the shear stress and the fibre and matrix relative displacement (Aveston and Kelly [10], Budiansky *et al.* [11], Leung and Li [12], and Li and Chan [13]). The present model follows the theory by Naaman *et al.* [5], and the relationship between the interface shear stress and the relative displacement between the fibre and the matrix is proposed to be linear.

0022–2461

With the model described below, the distributions of fibre and matrix stress, the interfacial shear stress, the strain difference between fibre and matrix, and the fibre relative displacement at the crack can be derived.

2. Single fibre

If a single fibre is analysed separately in the multiple cracking stage, some of the boundary conditions may be violated. It is usually assumed that when multiple cracking occurs, the crack widths are mutually equal. From the crack widths the unknown forces in the fibres at the crack can be obtained, at least by iteration. Once the fibre forces at the cracks are known, the composite stress can be evaluated.

Let the forces in the fibres at the cracks be known (Fig. 1). Following the pull-out theory by Naaman *et al.* [5] this leads to a second order differential equation for the fibre tensile force F

$$\frac{d^2F(x)}{dx^2} = -KP_1 + KQF(x) \tag{1}$$

where P_1 = fibre force at the crack

$$K = \frac{\psi\kappa}{A_mE_m} \tag{2}$$

$$Q = 1 + \frac{A_mE_m}{A_fE_f} \tag{3}$$

where κ = bond modulus, ψ = perimeter of fibre, A_f = cross-sectional area of fibre, A_m = area of matrix, E_f = modulus of elasticity of fibre and E_m = modulus of elasticity of matrix.
The bond modulus κ is defined by

$$\tau = \kappa S \tag{4}$$

where τ is the shear stress and S the relative displacement between the fibre and the matrix.

The matrix area is obtained from

$$\frac{A_m}{V_m} = \frac{A_f}{V_f} \tag{5}$$

where V_f and V_m are the volume contents of the fibres and the matrix, respectively.

The solution to Equation 1 is of the form

$$F = P_1\left(Ae^{\lambda x} + Be^{-\lambda x} + \frac{1}{Q}\right) \tag{6}$$

where

$$\lambda = (KQ)^{1/2} \tag{7}$$

The unknown coefficients can be determined from the following boundary conditions

$$F(0) = P_2 \tag{8}$$

$$F(l) = P_1 \tag{9}$$

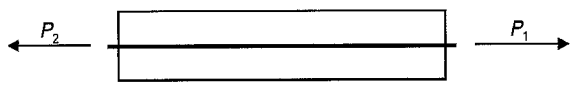

Figure 1 Single fibre.

where P_1 and P_2 are the fibre forces at the adjacent cracks and l is the segment length. This leads to

$$A = \frac{1}{1 - e^{-2\lambda l}}\left[\left(1 - \frac{1}{Q}\right)e^{-\lambda l} + \left(\frac{1}{Q} - \frac{P_2}{P_1}\right)e^{-2\lambda l}\right] \tag{10}$$

$$B = \frac{1}{1 - e^{-2\lambda l}}\left[-\left(1 - \frac{1}{Q}\right)e^{-\lambda l} - \left(\frac{1}{Q} - \frac{P_2}{P_1}\right)\right] \tag{11}$$

If P_2 is zero, the analysis is identical to that by Naaman *et al.* [5]. The shear stress between the fibre and the matrix is (according to [5]):

$$\tau = \frac{1}{\psi}\frac{dF}{dx} \tag{12}$$

and the local strain difference between the fibre and the matrix is:

$$\varepsilon_f - \varepsilon_m = \frac{1}{\psi\kappa}\frac{d^2F}{dx^2} \tag{13}$$

The relative fibre displacement at the crack can be derived using Equations 4 and 12:

$$\Delta = \frac{\tau(l)}{\kappa} = \frac{1}{\psi\kappa}\frac{dF}{dx}\bigg|_{x=l} = \frac{P_1\lambda}{\psi\kappa}(Ae^{\lambda l} - Be^{-\lambda l}) \tag{14}$$

It should be noted that in general one of the boundary conditions is violated at the crack where the fibre force is P_2. According to the previous analysis, the force in the matrix at the crack becomes $P_1 - P_2$, and not zero as it should be. In the following section a two-fibre system is introduced that satisfies all the boundary conditions.

3. Two-fibre system

Let us study two adjacent fibres that are symmetrically located so that the total force balance is satisfied at the crack (Fig. 2).

The equilibrium condition of the composite cross-section is

$$\begin{aligned} P &= F_1 + F_2 + T_1 + T_2 \\ &= (A_fE_f\varepsilon_f)_1 + (A_fE_f\varepsilon_f)_2 + (A_mE_m\varepsilon_m)_1 \\ &\quad + (A_mE_m\varepsilon_m)_2 \\ &= A_fE_f(\varepsilon_{f1} + \varepsilon_{f2}) + A_mE_m(\varepsilon_{m1} + \varepsilon_{m2}) \end{aligned} \tag{15}$$

where $P = P_1 + P_2$, F_i and T_i are the tensile forces in the fibre and the matrix, respectively, and the subscripts refer to either of the fibres and its

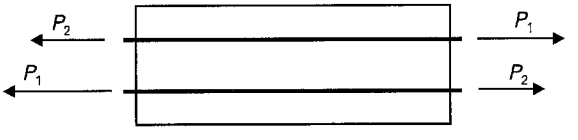

Figure 2 Two-fibre system.

surrounding matrix. The last equality in Equation 15 holds if the fibres are of the same type.

Let ε_m be defined as the average of the matrix strain around the two fibres

$$\varepsilon_m = \frac{1}{2}(\varepsilon_{m1} + \varepsilon_{m2}) \quad (16)$$

From Equations 15 and 16 it follows that

$$2\varepsilon_m = \frac{P}{A_m E_m} - \frac{A_f E_f}{A_m E_m}(\varepsilon_{f1} + \varepsilon_{f2}) \quad (17)$$

The local strain difference between the first fibre and the matrix is

$$\varepsilon_{f1} - \varepsilon_m = \frac{1}{2A_m E_m}\left[\left(\frac{2A_m E_m}{A_f E_f} + 1\right)F_1 - P + F_2\right] \quad (18)$$

Combining Equations 13 and 18, a second order differential equation for F_1 can be written

$$\frac{d^2F_1(x)}{dx^2} = -\hat{K}P + \hat{K}\hat{Q}F_1(x) + \hat{K}F_2(x) \quad (19)$$

where

$$\hat{K} = \frac{\psi\kappa}{2A_m E_m} \quad (20)$$

and

$$\hat{Q} = 1 + \frac{2A_m E_m}{A_f E_f} \quad (21)$$

A similar second order differential equation for F_2 is derived correspondingly

$$\frac{d^2F_2(x)}{dx^2} = -\hat{K}P + \hat{K}\hat{Q}F_2(x) + \hat{K}F_1(x) \quad (22)$$

Replacing F_2 in Equation 22 by its value extracted from Equation 19 gives

$$\frac{d^4F_1}{dx^4} - 2\hat{K}\hat{Q}\frac{d^2F_1(x)}{dx^2} + (\hat{Q}^2 - 1)\hat{K}^2F_1(x) = \hat{K}^2(\hat{Q} - 1)P \quad (23)$$

Equation 23 is a fourth order differential equation for F_1. The solution to this differential equation is of the form

$$F_1(x) = Ae^{-\lambda_1 x} + Be^{\lambda_1 x} + Ce^{-\lambda_2 x} + De^{\lambda_2 x} + \frac{P}{\hat{Q} + 1} \quad (24)$$

where

$$\lambda_1 = [\hat{K}(\hat{Q} - 1)]^{1/2} \quad (25)$$

$$\lambda_2 = [\hat{K}(\hat{Q} + 1)]^{1/2} \quad (26)$$

It can be shown that λ_2 is the same as λ in Equation 7. F_2 can be obtained from Equation 19 as

$$F_2(x) = -Ae^{-\lambda_1 x} - Be^{\lambda_1 x} + Ce^{-\lambda_2 x} + De^{\lambda_2 x} + \frac{P}{\hat{Q} + 1} \quad (27)$$

The unknown coefficients are determined from the following boundary conditions (see Fig. 2)

$$F_1(0) = P_1 \quad (28)$$

$$F_1(l) = P_2 \quad (29)$$

$$F_2(0) = P_2 \quad (30)$$

$$F_2(l) = P_1 \quad (31)$$

Using Equations 24 and 27, Equations 28–31 can be written in matrix form

$$\begin{bmatrix} 1 & 1 & 1 & 1 \\ e^{-\lambda_1 l} & e^{\lambda_1 l} & e^{-\lambda_2 l} & e^{\lambda_2 l} \\ -1 & -1 & 1 & 1 \\ -e^{-\lambda_1 l} & -e^{\lambda_1 l} & e^{-\lambda_2 l} & e^{\lambda_2 l} \end{bmatrix} \begin{Bmatrix} A \\ B \\ C \\ D \end{Bmatrix} = \begin{Bmatrix} P_1 - P/(\hat{Q} + 1) \\ P_2 - P/(\hat{Q} + 1) \\ P_2 - P/(\hat{Q} + 1) \\ P_1 - P/(\hat{Q} + 1) \end{Bmatrix} \quad (32)$$

The unknown coefficients are solved from Equation 32

$$A = \frac{P_1 - P_2}{2(1 - e^{-\lambda_1 l})} \quad (33)$$

$$B = \frac{-P_1 + P_2}{2e^{\lambda_1 l}(1 - e^{-\lambda_1 l})} \quad (34)$$

$$C = \frac{(\hat{Q} - 1)(P_1 + P_2)}{2(1 + e^{-\lambda_2 l})(\hat{Q} + 1)} \quad (35)$$

$$D = \frac{(\hat{Q} - 1)(P_1 + P_2)}{2e^{\lambda_2 l}(1 + e^{-\lambda_2 l})(\hat{Q} + 1)} \quad (36)$$

The relative fibre displacement at the crack is:

$$\Delta = \frac{1}{\psi\kappa}\frac{dF_2}{dx}\bigg|_{x=l} = \frac{1}{\psi\kappa} \times (\lambda_1 Ae^{-\lambda_1 l} - \lambda_1 Be^{\lambda_1 l} - \lambda_2 Ce^{-\lambda_2 l} + \lambda_2 De^{\lambda_2 l}) \quad (37)$$

3.1 Fibres shorter than the segment between cracks

If the fibre does not extend over the adjacent crack but the embedded end lies within the segment between two cracks (Fig. 3(a)), the boundary conditions differ from the previous analysis. As can be seen in Fig. 3(a), there are four fibres instead of two, as statistically the fibre volume content must be the same throughout the composite. In Fig. 3 the lower fibres are symmetrical to the upper fibres.

The analysis can be divided into three steps by superposition (Fig. 3(b)). The first two steps can be analysed separately with a single fibre analysis, since the boundary conditions are satisfied. The third step is analysed below. It should be noted that the superposition is not strictly valid and does not lead to exactly the same results as without superposition. This is due to the fact that the first two cases in Fig. 3(b) are not mutually independent but would instead have some interaction.

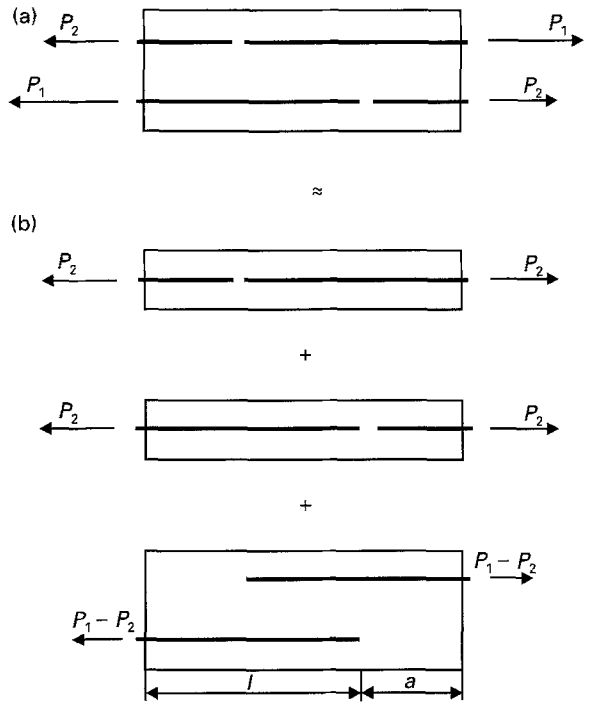

Figure 3 The two fibres partially overlap within the segment between two cracks. The analysis is divided into three steps by the superposition method.

In the first region ($0 \leqslant x \leqslant a$) there is only one load-carrying fibre, and the corresponding matrix area is twice as large as normal. The fibre force can be obtained with a single fibre analysis replacing the matrix area A_m by $2A_m$. In the middle of the segment ($a \leqslant x \leqslant l$), the analysis of a two-fibre system is performed. Let F_1 and F_2 be the forces in the lower and upper fibres, respectively. They can be written in the form

$$F_1 = \begin{cases} Ae^{\hat{\lambda}x} + Be^{-\hat{\lambda}x} + R/\hat{Q}, & 0 \leqslant x \leqslant a \\ Ce^{-\lambda_1 x} + De^{\lambda_1 x} + Ee^{-\lambda_2 x} + Fe^{\lambda_2 x} + R/(\hat{Q}+1), & a < x \leqslant l \\ 0, & l < x \leqslant a + l \end{cases} \quad (38)$$

$$F_2 = \begin{cases} 0, & 0 \leqslant x \leqslant a \\ -Ce^{-\lambda_1 x} - De^{\lambda_1 x} + Ee^{-\lambda_2 x} + Fe^{\lambda_2 x} + R/(\hat{Q}+1), & a < x \leqslant l \\ Ge^{\hat{\lambda}x} + He^{-\hat{\lambda}x} + R/\hat{Q}, & l < x \leqslant a + l \end{cases} \quad (39)$$

where

$$\hat{\lambda} = (\hat{K}\hat{Q})^{1/2} \quad (40)$$

and

$$R = P_1 - P_2 \quad (41)$$

The boundary and compatibility conditions are

$$F_1(0) = R \quad (42)$$

$$F_1(a^-) = F_1(a^+) \quad (43)$$

$$F_1'(a^-) = F_1'(a^+) \quad (44)$$

$$F_1(s) = F_2(s) \quad (45)$$

$$F_1'(s) = -F_2'(s) \quad (46)$$

$$F_2(a) = 0 \quad (47)$$

where $s = (a + l)/2$. Note that symmetry conditions have been used. The shear stress between the fibre and the matrix must be continuous, as it has been assumed that the relative displacement between the fibre and the matrix is proportional to the shear stress and must therefore be continuous.

The unknown coefficients can be determined from the following simultaneous equations written in matrix form

$$\begin{bmatrix} 1 & 1 & 0 & 0 & 0 & 0 \\ -e^{-\hat{\lambda}a} & -e^{\hat{\lambda}a} & e^{-\lambda_1 a} & e^{\lambda_1 a} & e^{-\lambda_2 a} & e^{\lambda_2 a} \\ \hat{\lambda}e^{-\hat{\lambda}a} & -\hat{\lambda}e^{\hat{\lambda}a} & -\lambda_1 e^{-\lambda_1 a} & \lambda_1 e^{\lambda_1 a} & -\lambda_2 e^{-\lambda_2 a} & \lambda_2 e^{\lambda_2 a} \\ 0 & 0 & e^{-\lambda_1 s} & e^{\lambda_1 s} & 0 & 0 \\ 0 & 0 & e^{-\lambda_1 a} & e^{\lambda_1 a} & -e^{-\lambda_2 a} & -e^{\lambda_2 a} \\ 0 & 0 & 0 & 0 & -\lambda_2 e^{-\lambda_2 s} & \lambda_2 e^{\lambda_2 s} \end{bmatrix}$$

$$\begin{Bmatrix} A \\ B \\ C \\ D \\ E \\ F \end{Bmatrix} = \begin{Bmatrix} R - R/\hat{Q} \\ R/(\hat{Q}+1) \\ 0 \\ 0 \\ R/(\hat{Q}+1) \\ 0 \end{Bmatrix} \quad (48)$$

The matrix Equation 48 can be solved numerically.

The relative fibre displacement at the crack can be evaluated by

$$\Delta = \frac{1}{\psi\kappa}\frac{dF_1}{dx}\bigg|_{x=0} \quad (49)$$

Δ now being negative because the fibre moves to the left.

4. Comparison of single-fibre and two-fibre system theories

To compare the analyses of the single- and two-fibre systems, some numerical cases were performed. The following material parameters were chosen: fibre diameter $d = 1$ mm, $V_f = 5\%$, $E_f = 210$ GPa, $E_m = 21$ GPa, and $\kappa = 1.2 \times 10^{13}$ N m^{-3}. The fibre forces at the cracks are assumed to be known.

4.1 Case 1

Let the segment length between the two cracks be $l = 30$ mm, and the fibre forces at the cracks be $P_1 = 100$ N and $P_2 = 0$. The distributions of the fibre force, interfacial shear stress and strain difference between the fibre and the matrix are shown in Fig. 4.

The solid lines represent the two-fibre system and the dashed lines the single-fibre system. For the single fibre system the relative displacement is $\Delta = 1.027 \times 10^{-3}$ mm and for the two-fibre system it is $\Delta = 1.147 \times 10^{-3}$ mm, the relative error being 10.5%.

From Fig. 4 it can be seen that when the fibre force is nearly constant, its value in the single-fibre analysis is twice that obtained in the two-fibre system analysis. The reason is seen in Fig. 5. In both analyses, the total matrix force distributions are equal. The matrix force was derived by $T(x) = P - F_1(x) - F_2(x)$. In the two-fibre system the fibre force distributions are symmetrical, while in a single fibre analysis they are not due to the violated boundary conditions. Therefore the two-fibre system analysis is believed to give more accurate results for the fibre displacement at the crack.

4.2 Case 2

Let the segment length between the two cracks be $l = 30$ mm, and the fibre forces at the cracks be $P_1 = 100$ N and $P_2 = 70$ N. The distributions of the fibre force, interfacial shear stress and strain difference between the fibre and the matrix are shown in Fig. 6. For the single fibre system the relative displacement is $\Delta = 1.027 \times 10^{-3}$ mm and for the two-fibre system it is $\Delta = 1.063 \times 10^{-3}$ mm, the relative error being 3.4%.

4.3 Case 3

Let the segment length between the two cracks be $l = 5$ mm, and the fibre forces at the cracks be $P_1 = 100$ N and $P_2 = 0$. The distributions of the fibre force, interfacial shear stress and strain difference between the fibre and the matrix are shown in Fig. 7.

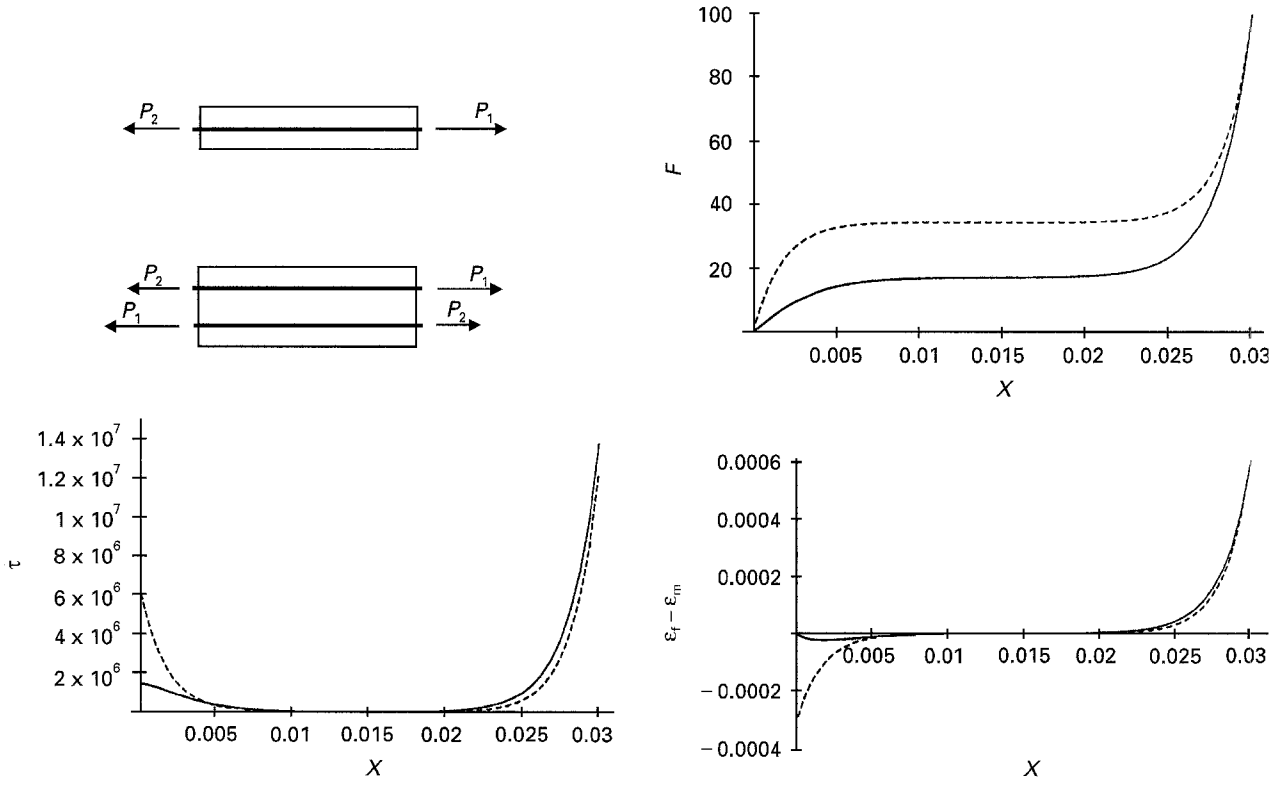

Figure 4 Distributions of fibre force, interfacial shear stress and strain difference between fibre and matrix. Solid lines: two-fibre system; dashed lines: single fibre system. $l = 30$ mm, $P_1 = 100$ N and $P_2 = 0$.

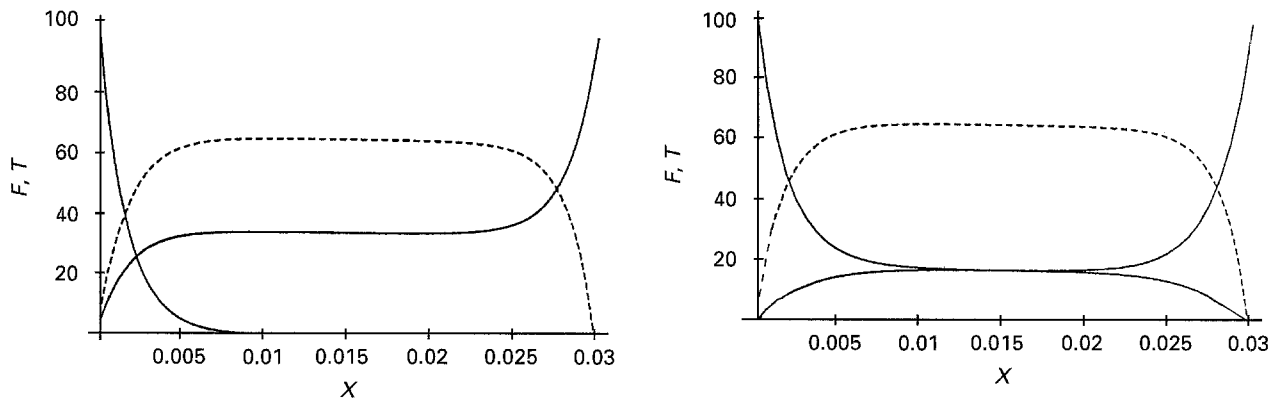

Figure 5 Distributions of fibre forces and total matrix force. (a) Single fibre system with two cases separately analysed: $P_1 = 100$ N, $P_2 = 0$, and $P_1 = 0$, $P_2 = 100$ N. (b) Two-fibre system with $P_1 = 100$ N, $P_2 = 0$. Solid lines: fibre forces; dashed lines: matrix force, $l = 30$ mm.

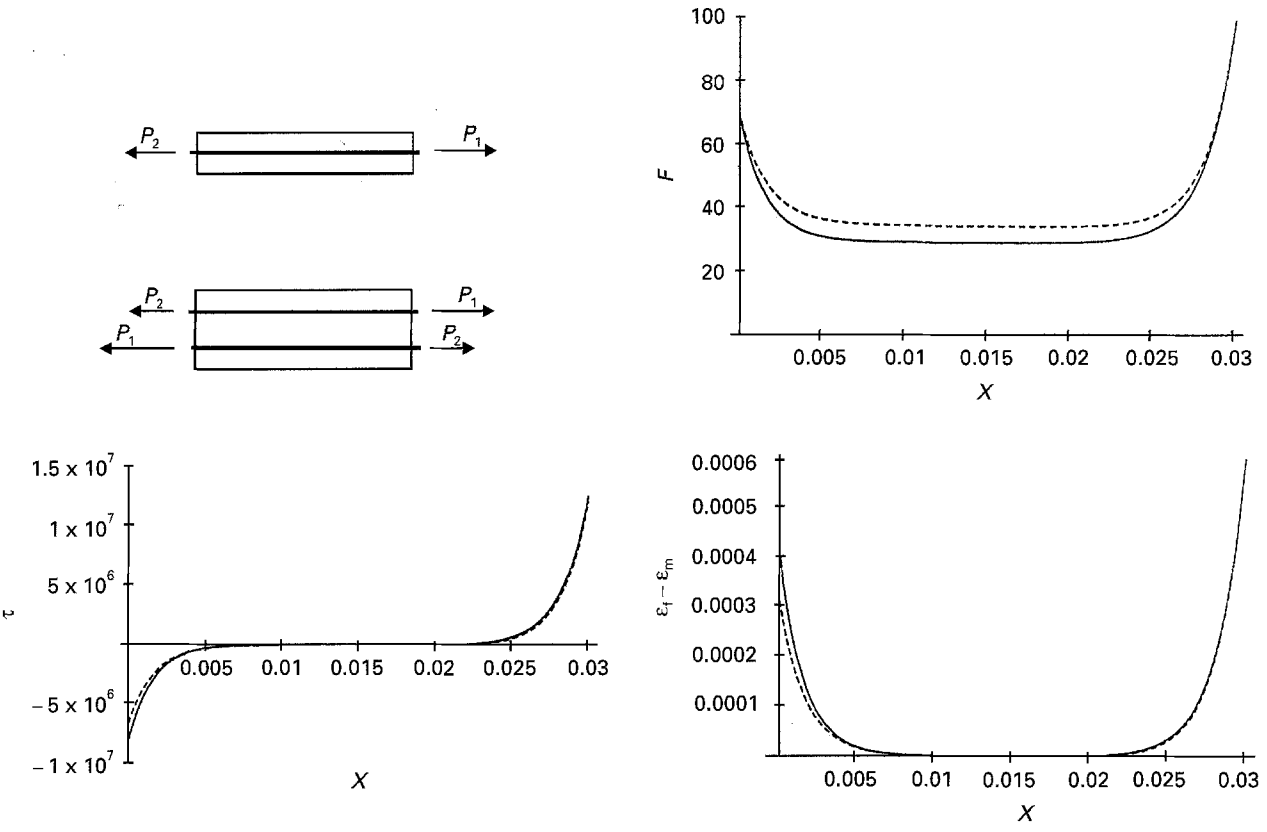

Figure 6 Distributions of fibre force, interfacial shear stress and strain difference between fibre and matrix. Solid lines: two-fibre system; dashed lines: single fibre system. $l = 30$ mm, $P_1 = 100$ N and $P_2 = 70$ N.

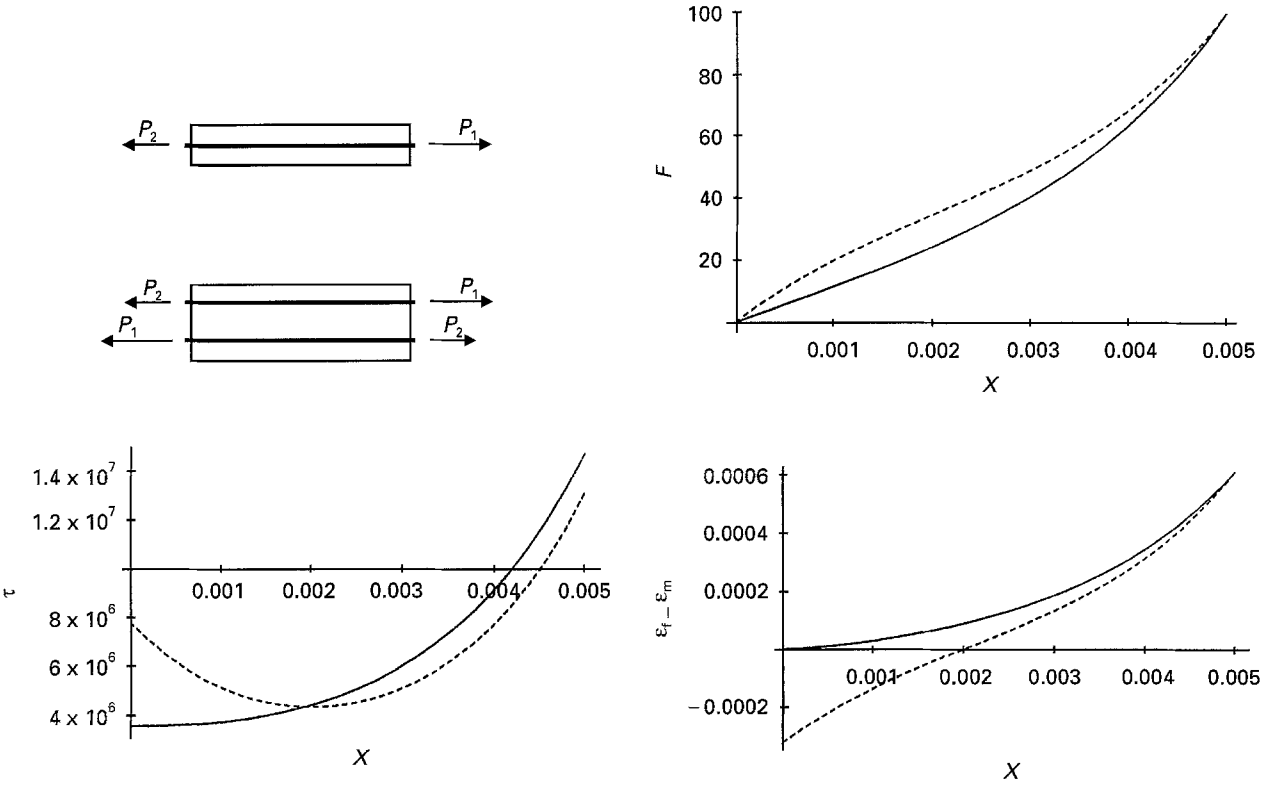

Figure 7 Distributions of fibre force, interfacial shear stress and strain difference between fibre and matrix. Solid lines: two-fibre system; dashed lines: single fibre system. $l = 5$ mm, $P_1 = 100$ N and $P_2 = 0$.

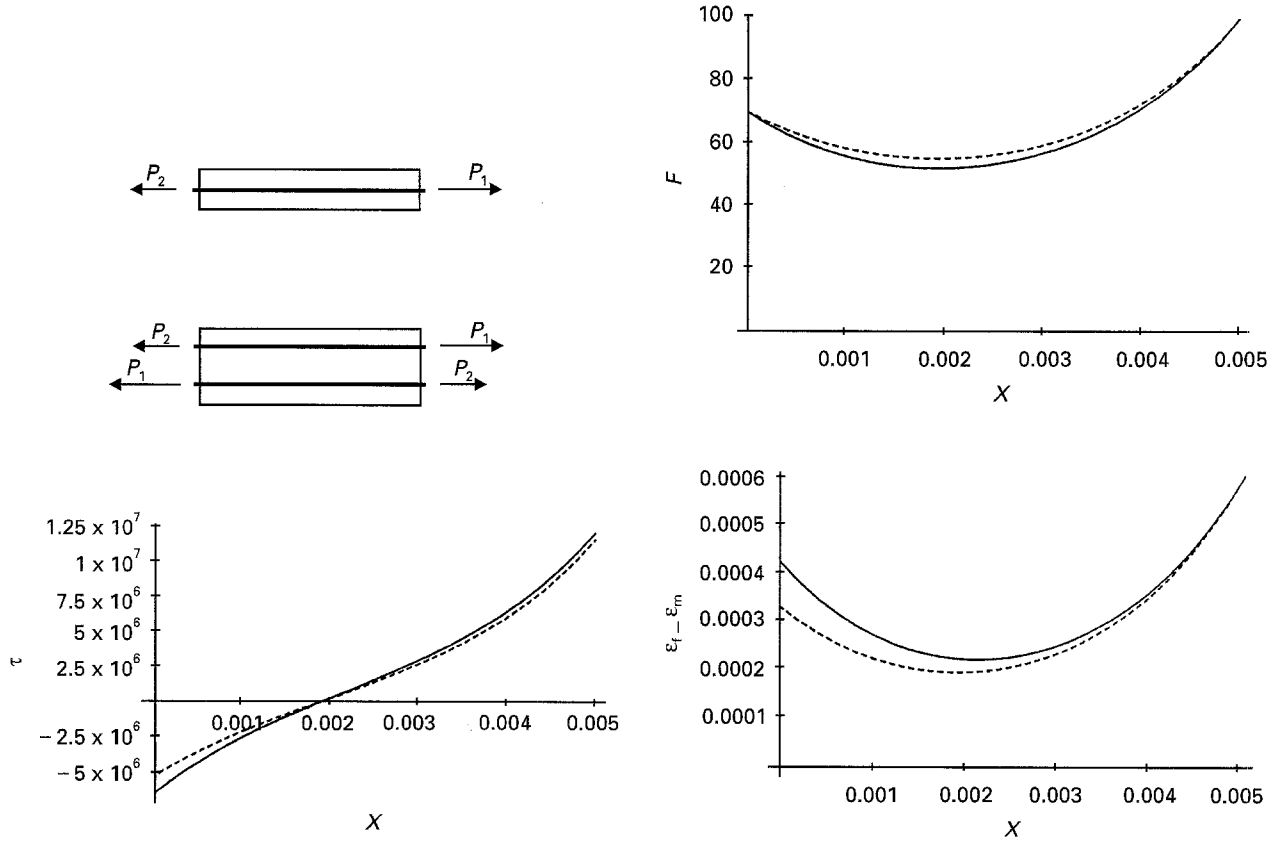

Figure 8 Distributions of fibre force, interfacial shear stress and strain difference between fibre and matrix. Solid lines: two-fibre system; dashed lines: single fibre system. $l = 5$ mm, $P_1 = 100$ N and $P_2 = 70$ N.

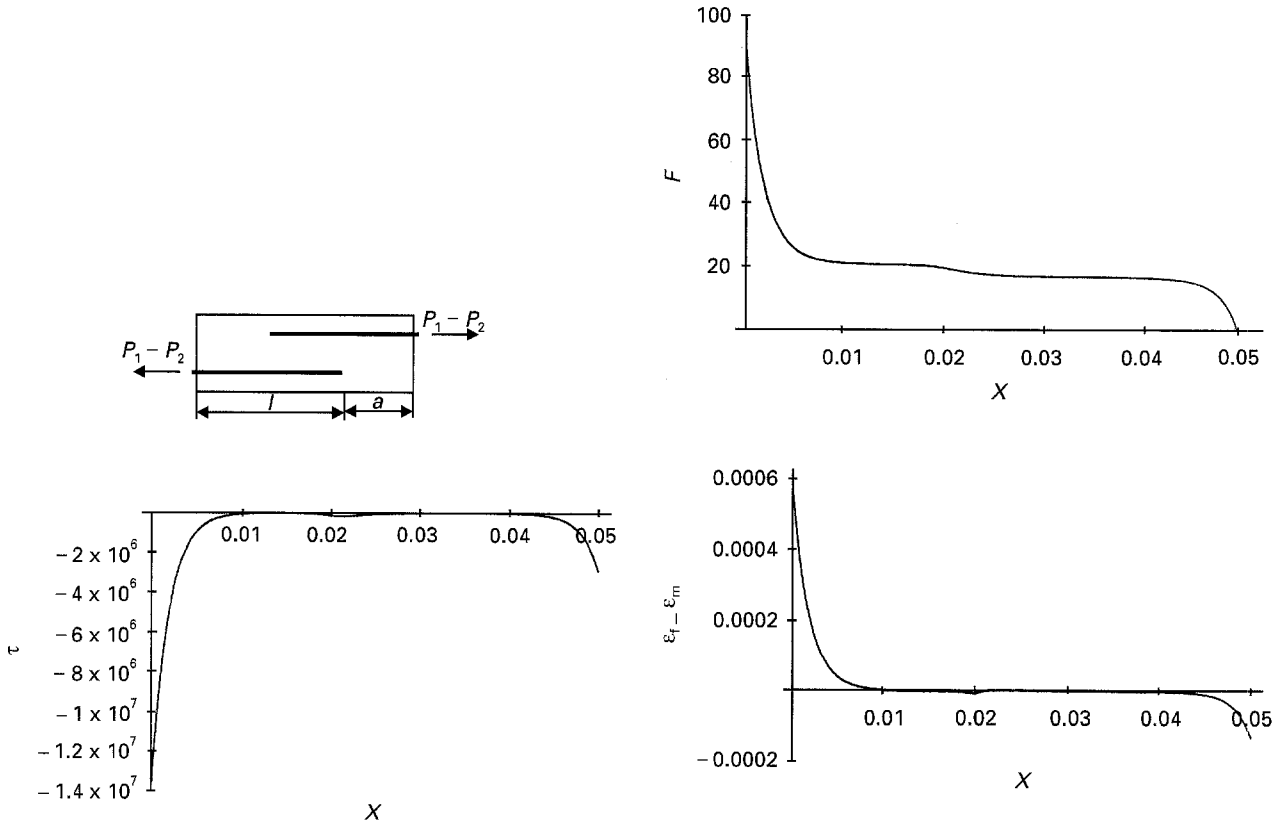

Figure 9 Distribution of fibre force interfacial shear stress and strain difference between fibre and matrix. $P_1 - P_2 = 100$ N.

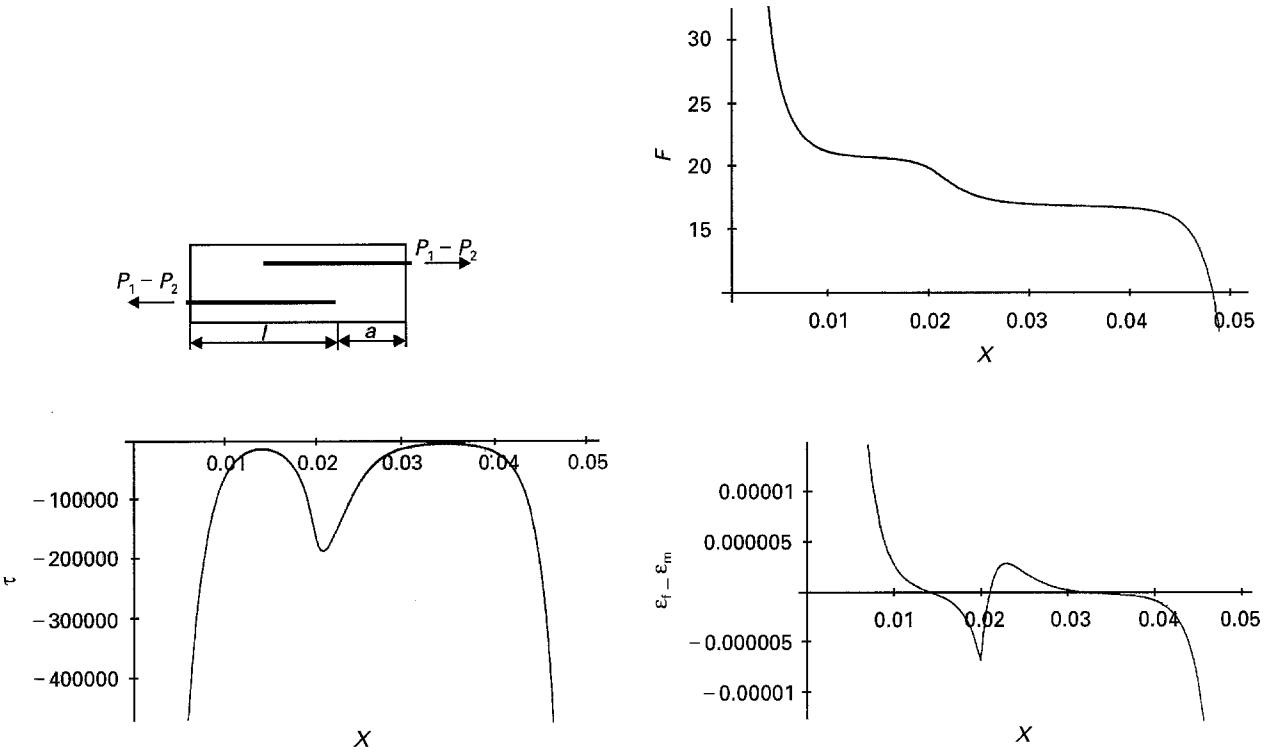

Figure 10 Distributions of fibre force, interfacial shear stress and strain difference between fibre and matrix at the symmetry fibre end region. $P_1 - P_2 = 100$ N.

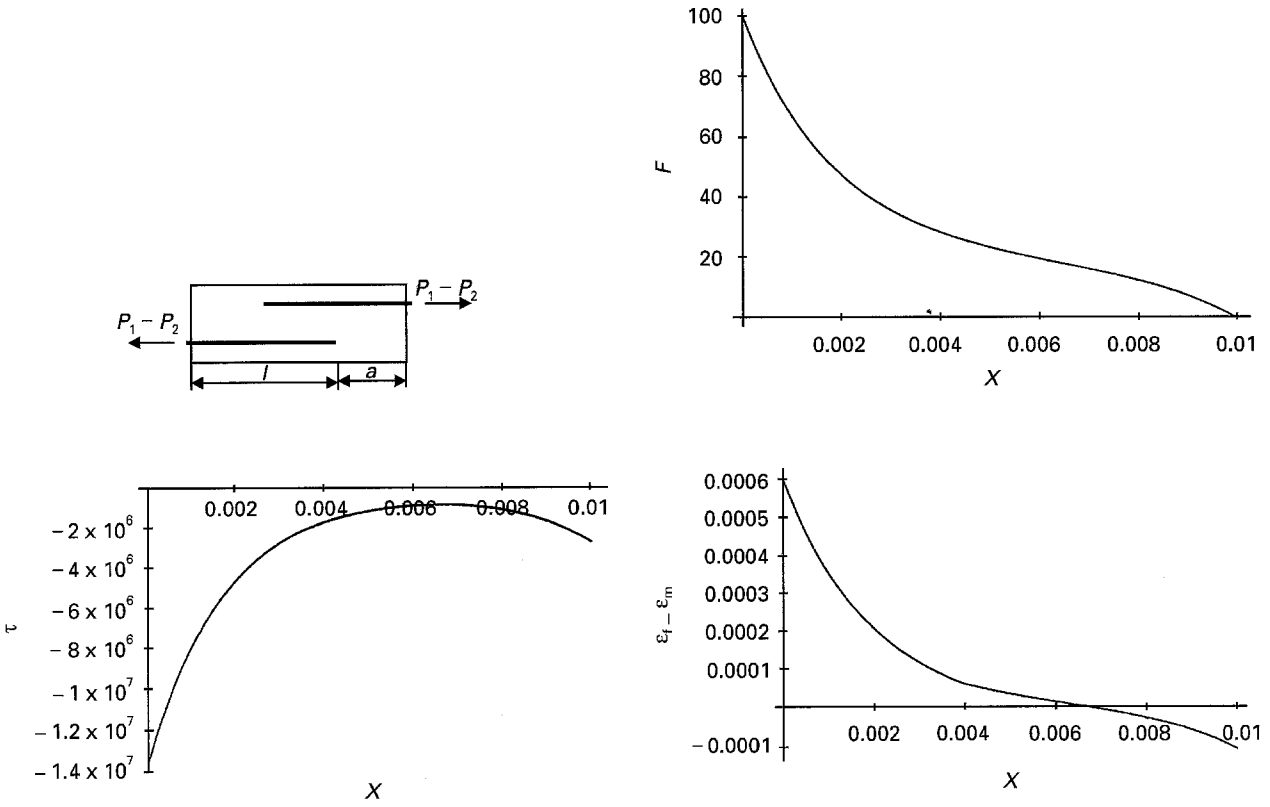

Figure 11 Distributions of fibre force, interfacial shear stress and strain difference between fibre and matrix. $P_1 - P_2 = 100$ N.

For the single fibre system the relative displacement is $\Delta = 1.089 \times 10^{-3}$ mm and for the two-fibre system it is $\Delta = 1.224 \times 10^{-3}$ mm, the relative error being 11.0%.

4.4 Case 4

Let the segment length between the two cracks be $l = 5$ mm, and the fibre forces at the cracks be $P_1 = 100$ N and $P_2 = 70$ N. The distributions of the

fibre force, interfacial shear stress and strain difference between the fibre and the matrix are shown in Fig. 8. For the single fibre system the relative displacement is $\Delta = 0.974 \times 10^{-3}$ mm and for the two-fibre system it is $\Delta = 1.015 \times 10^{-3}$ mm, the relative error being 4.0%.

5. Examples of fibres shorter than the segment between cracks

A two-fibre system is now analysed with the fibres partially overlapping within the segment between two cracks (Fig. 3(b)). The material parameters are as above. The fibre force at the crack is $R = P_1 - P_2 = 100$ N.

5.1 Case 5

The fibre embedded length is $l = 50$ mm, and the crack spacing is 70 mm, or $a = 20$ mm (see Fig. 3). The fibre force, shear stress at the interface, and strain difference distributions are shown in Fig. 9. In Fig. 10 the same quantities are shown at the end region of the symmetry fibre. It can be seen that the force distribution in the fibre is nearly constant at two intervals, and that the strain difference between the fibre and matrix reaches zero three times. The relative displacement at the crack is $\Delta = 1.128 \times 10^{-3}$ mm.

5.2 Case 6

The fibre embedded length is $l = 10$ mm, and the crack spacing is 14 mm, or $a = 4$ mm (see Fig. 3). The fibre force, shear stress at the interface, and strain difference distributions are shown in Fig. 11. It can be seen that the strain difference reaches zero only in the region where the two fibres overlap. The relative displacement at the crack is $\Delta = 1.134 \times 10^{-3}$ mm.

6. Concluding remarks

A fibre pull-out problem in the multiple cracking stage was studied. Full bonding was assumed. To satisfy the equilibrium conditions at the cracks, a symmetry fibre was assumed to be located at the adjacent crack symmetrically to the fibre being analysed. This assumption can be used in the statistical analysis of a multiple cracked composite. Analysing the two-fibre system leads to more complex formulae than for a single fibre system, but equilibrium conditions are satisfied. Thus the displacement derived from the two-fibre system analysis is believed to be more accurate than that obtained from the single fibre analysis.

Comparing the solutions of the single and two-fibre systems showed that the latter gave a greater displacement at the crack. The maximum relative difference was 11%.

The most complicated case, in which the two fibres partially overlap between the cracks, was analysed and two examples were presented. The distributions of fibre force, the interfacial shear stress, and the strain difference between the fibre and the matrix were seen to depend on the crack spacing.

To apply the present theory to real composites, the fibre forces at the cracks should be derived from the crack widths, which may require an iteration routine. Moreover, a theory of debonding fibres in the multiple cracking case is still to be developed.

Acknowledgements

This study was supported by the Academy of Finland and the Technical Research Centre of Finland. This support is gratefully acknowledged.

Appendix 1. Notation

The following symbols are used in this paper

A_f = area of fibre
A_m = area of matrix
E_f = modulus of elasticity of fibre
E_m = modulus of elasticity of matrix
F, F_1, F_2 = tensile forces in fibres
$K = \dfrac{\psi\kappa}{A_m E_m}$
$\hat{K} = \dfrac{\psi\kappa}{2A_m E_m}$
l = fibre embedded length or segment length
P, P_1, P_2 = fibre forces at the cracks
$Q = 1 + \dfrac{A_m E_m}{A_f E_f}$
$\hat{Q} = 1 + \dfrac{2A_m E_m}{A_f E_f}$
$R = P_1 - P_2$
S = slip between fibre and matrix
T, T_1, T_2 = tensile forces in matrix
V_f = fibre volume fraction
$V_m = 1 - V_f$ = matrix volume fraction
Δ = displacement of fibre free end
κ = bond modulus
$\lambda = (KQ)^{1/2}$
$\hat{\lambda} = (\hat{K}\hat{Q})^{1/2}$
$\lambda_1 = [\hat{K}(\hat{Q} - 1)]^{1/2}$
$\lambda_2 = [\hat{K}(\hat{Q} + 1)]^{1/2}$
ψ = perimeter of fibre
τ = shear stress between fibre and matrix

References

1. A. E. NAAMAN and S. P. SHAH, in Proceedings of the 11th National Symposium on Fracture Mechanics, edited by C. W. Smith and S. W. Freiman (ASTM 1979), p. 183.
2. P. TJIPTOBROTO and W. HANSEN, *ACI Mater. J.* **90** (1993) 16.
3. V. C. LI and C. K. Y. LEUNG, *J. Engng. Mech.* **118** (1992) 2246.
4. J. KULLAA, *Composites* **25** (1994) 935.
5. A. E. NAAMAN, G. G. NAMUR, J. M. ALWAN and H. S. NAJM, *J. Struct. Engng.* **117** (1991) 2769.
6. J. AVESTON, G. A. COOPER and A. KELLY, in Proceeding Conference National Physical Laboratories, 4 November 1971, Guildford. (IPC Science and Technology Press Ltd, 1971) p. 15.
7. G. Jr. NAMMUR and A. E. NAAMAN, *ACI Mater. J.* **86** (1989) 45.

8. T. Y. LIM, P. PARAMASIVAM and S. L. LEE, *Ibid.* **84** (1987) 286.
9. H. STANG, Z. LI and S. P. SHAH, *J. Engng. Mech.* **116** (1990) 2136.
10. J. AVESTON and A. KELLY, *J. Mater. Sci.* **8** (1973) 352.
11. B. BUDIANSKY, J. W. HUTCHINSON and A. G. EVANS, *J. Mech. Phys. Solids* **34** (1986) 167.
12. C. K. Y. LEUNG, V. C. LI, *Composites* **21** (1990) 305.
13. V. C. LI and Y.-W. CHAN, *J. Engng. Mech.* **120** (1994) 707.

Received 10 March
and accepted 16 August 1995